



# Kaposi's sarcoma herpesvirus is associated with osteosarcoma in Xinjiang populations

Qian Chen<sup>a,1</sup>, Jiangtao Chen<sup>b,1</sup>, Yuqing Li<sup>a,1,2</sup>, Dawei Liu<sup>c</sup>, Yan Zeng<sup>d</sup>, Zheng Tian<sup>b</sup>, Akbar Yunus<sup>b</sup>, Yong Yang<sup>b</sup>, Jie Lu<sup>e</sup>, Xinghua Song<sup>b,3,4</sup>, and Yan Yuan<sup>a,e,4</sup>

<sup>a</sup>Institute of Human Virology, Zhongshan School of Medicine, Sun Yat-Sen University, Guangzhou, Guangdong 510080, China; <sup>b</sup>First Affiliated Hospital, Xinjiang Medical University, Urumqi, Xinjiang Uyghur Autonomous Region, 830011, China; <sup>c</sup>Department of Pathology, The First Affiliated Hospital, Sun Yat-sen University, Guangzhou, Guangdong 510080, China; <sup>d</sup>Shihezi University, Shihezi, Xinjiang Uyghur Autonomous Region, 832000, China; and <sup>e</sup>Department of Basic and Translational Sciences, University of Pennsylvania School of Dental Medicine, Philadelphia, PA 19104

Edited by Yuan Chang, University of Pittsburgh, Pittsburgh, PA, and approved February 3, 2021 (received for review August 6, 2020)

**Osteosarcoma is the most common malignant tumor of bone predominately affecting adolescents and young adults. Based on animal studies, a viral etiology of osteosarcoma was proposed more than a half-century ago, but no viral association with human osteosarcoma has been found. The Uyghur ethnic population in Xinjiang, China, has an unusually high prevalence of Kaposi's sarcoma-associated herpesvirus (KSHV) infection and elevated incidence of osteosarcoma. In the current study, we explored the possible association of KSHV infection and osteosarcoma occurrence. Our seroepidemiological study revealed that KSHV prevalence was significantly elevated in Uyghur osteosarcoma patients versus the general Uyghur population (OR, 10.23; 95%CI, 4.25, 18.89). The KSHV DNA genome and viral latent nuclear antigen LANA were detected in most osteosarcoma tumor cells. Gene expression profiling analysis showed that KSHV-positive osteosarcoma represents a distinct subtype of osteosarcomas with viral gene-activated signaling pathways important for osteosarcoma development. We conclude that KSHV infection is a risk factor for osteosarcoma, and KSHV is associated with some osteosarcomas, representing a newly identified viral-associated endemic cancer.**

Kaposi's sarcoma-associated herpesvirus | human herpesvirus type 8 | osteosarcoma | seroepidemiology | viral-associated endemic cancer

Osteosarcoma is the most common malignant tumor of bone with an incidence of approximately three cases per million annually worldwide, predominately affecting adolescents and young adults, with a major peak between 10 and 14 y old and a second smaller peak in the geriatric population (1, 2). Osteosarcomas have a rather heterogeneous genetic profile and lack any consistent unifying event that leads to its pathogenesis. It may result from oncogenic events sustained by cells in the differentiation lineage hierarchy from mesenchymal stem cells through to osteoblast. Still, it may also suggest that osteosarcoma could arise with multiple etiologies and different pathogenesis. Concerning the etiology of osteosarcoma, three primary potential etiological agents, namely chemical agents, physical agents, and viruses, are believed to associate with osteosarcoma. Numerous chemicals are known to induce osteosarcoma such as beryllium and methylcholanthrene (3, 4). Radiation exposure is also related to osteosarcoma development (5, 6). A viral etiology for osteosarcoma has been suggested since Finkel isolated viruses from mice that produced similar tumors when injected into newborn mice (7). There was also evidence of a bone tumor virus in the human disease, as injection of cell-free extracts of human bone cancer into newborn Syrian hamsters induced various mesenchymal tumors including osteosarcoma (8). However, the viral etiology has never been proven by the identification of any virus that is authentically associated with human osteosarcoma. The current study aimed to explore whether any human osteosarcoma is associated with a viral infection.

Kaposi's sarcoma-associated herpesvirus (KSHV), also termed human herpesvirus type 8, was first identified in Kaposi's sarcoma (KS) lesions in 1994 (9). KSHV can be found in almost 100% of KS lesions, regardless of their source or clinical subtype (i.e., classic, AIDS-associated, African endemic, or posttransplant KS). Additionally, KSHV is also associated with two lymphoproliferative diseases, namely primary effusion lymphoma and multicentric Castleman's disease (10–12). We and others showed that human mesenchymal stem cells (MSCs) are highly susceptible to KSHV infection, and infection promotes multilineage (osteogenic, adipogenic, and angiogenic) differentiation (13–15). Several lines of evidence suggest that the KSHV infection of MSCs leads to KS through a mesenchymal-to-endothelial transition process (13, 16).

Given that osteosarcomas originate from mesenchymal stem cells or their immediate lineage progenitors (17, 18) and KSHV can effectively infect MSCs and drive osteogenic differentiation (13), the question was raised whether KSHV infection of MSCs

## Significance

**A viral etiology of osteosarcoma was proposed previously but has never been proven by identifying any virus authentically associated with human osteosarcoma. The current study revealed an association of human osteosarcoma with KSHV infection in osteosarcoma patients of Xinjiang subgroups. First, this study provides evidence that supports a viral etiology of some human osteosarcomas. The gene expression profiling study showed that KSHV-positive osteosarcoma represents a distinct subtype of osteosarcoma which is of diagnostic, prognostic, and therapeutic significance. Second, KSHV-associated osteosarcomas occur preferentially in children and young adults, predicting that KSHV-positive children in KSHV-endemic regions may be at significant risk for osteosarcoma. Third, these findings extend the range of human cancers associated with viruses.**

Author contributions: Q.C., Y.L., Y.Z., X.S., and Y. Yuan designed research; Q.C., J.C., and Y.L. performed research; J.C., D.L., Y.Z., Z.T., A.Y., Y. Yang, and X.S. contributed new reagents/analytic tools; Q.C., Y.L., D.L., Y.Z., J.L., and Y. Yuan analyzed data; and Y. Yuan wrote the paper.

The authors declare no competing interest.

This article is a PNAS Direct Submission.

Published under the PNAS license.

<sup>1</sup>Q.C., J.C., and Y.L. contributed equally to this work.

<sup>2</sup>Present address: Department of Urological Surgery, Affiliated Luohu Hospital, Shenzhen University, Shenzhen, Guangdong 518000, China.

<sup>3</sup>Present address: The Orthopedic Department, The First Affiliated Hospital of Jinan University, Guangzhou, Guangdong 510630, China.

<sup>4</sup>To whom correspondence may be addressed. Email: yuan2@upenn.edu or songxinghua19@163.com.

This article contains supporting information online at <https://www.pnas.org/lookup/suppl/doi:10.1073/pnas.2016653118/-DCSupplemental>.

Published March 5, 2021.

contributes to osteosarcoma development. To this end, we investigated the association of KSHV infection and osteosarcoma occurrence in the ethnic Uyghur population in Xinjiang Uyghur autonomous region of China, where there is a high seroprevalence of KSHV, a high incidence of KS, and a high occurrence of osteosarcoma among the Uyghur population (19–21). We found that the seroprevalence of KSHV in Uyghur osteosarcoma patients is significantly higher than that of the Uyghur general population. KSHV genomic DNA and viral latent nuclear antigen (LANA) were detected in osteosarcoma tumors of most of the patients who were KSHV seropositive. Furthermore, gene expression profile analysis of osteosarcoma clinical samples demonstrated that KSHV infection regulates the genes and signaling pathways essential for osteosarcoma development. These results revealed a strong association between KSHV infection and osteosarcoma.

## Results

**Seroepidemiological Evidence for Association of KSHV Infection with Osteosarcoma in Xinjiang Uyghur Ethnic Population.** Xinjiang, China, is an endemic area for KS, and classic KS is prevalent among the ethnic Uyghur population (19). The seroprevalence

of KSHV among the Xinjiang Uyghur population is unusually high, ranging from 20.7 to 40.4% compared to that of the general population of China (11.3%) (20). It is striking that although the Uyghurs account for 45% of the total Xinjiang population (according to the 2010 Census of Xinjiang), the majority of osteosarcoma patients diagnosed in our hospital (First Affiliated Hospital, Xinjiang Medical University) happened to be Uyghurs. It raised a question if KSHV infection is associated with at least some osteosarcomas. To obtain epidemiological evidence regarding this, we compared the KSHV seroprevalence between osteosarcoma patients and the general population. A diagnostic enzyme-linked immunosorbent assay (ELISA) was developed with three recombinant proteins of KSHV, namely LANA, ORF65, and K8.1, and used to examine sera of 21 Uyghur osteosarcoma patients and 327 control individuals (the general Uyghur population). Seventeen of 21 (81%) Uyghur osteosarcoma patients were found seropositive to at least one of the KSHV antigens (*SI Appendix, Table S1*). The serum samples of osteosarcoma patients were also examined in a blinded fashion by an immunofluorescence assay with BCBL-1 cells, and LANA nuclear staining with distinctive punctate dots was detected with sera of 17 out of 21 patients, consistent with the ELISA results

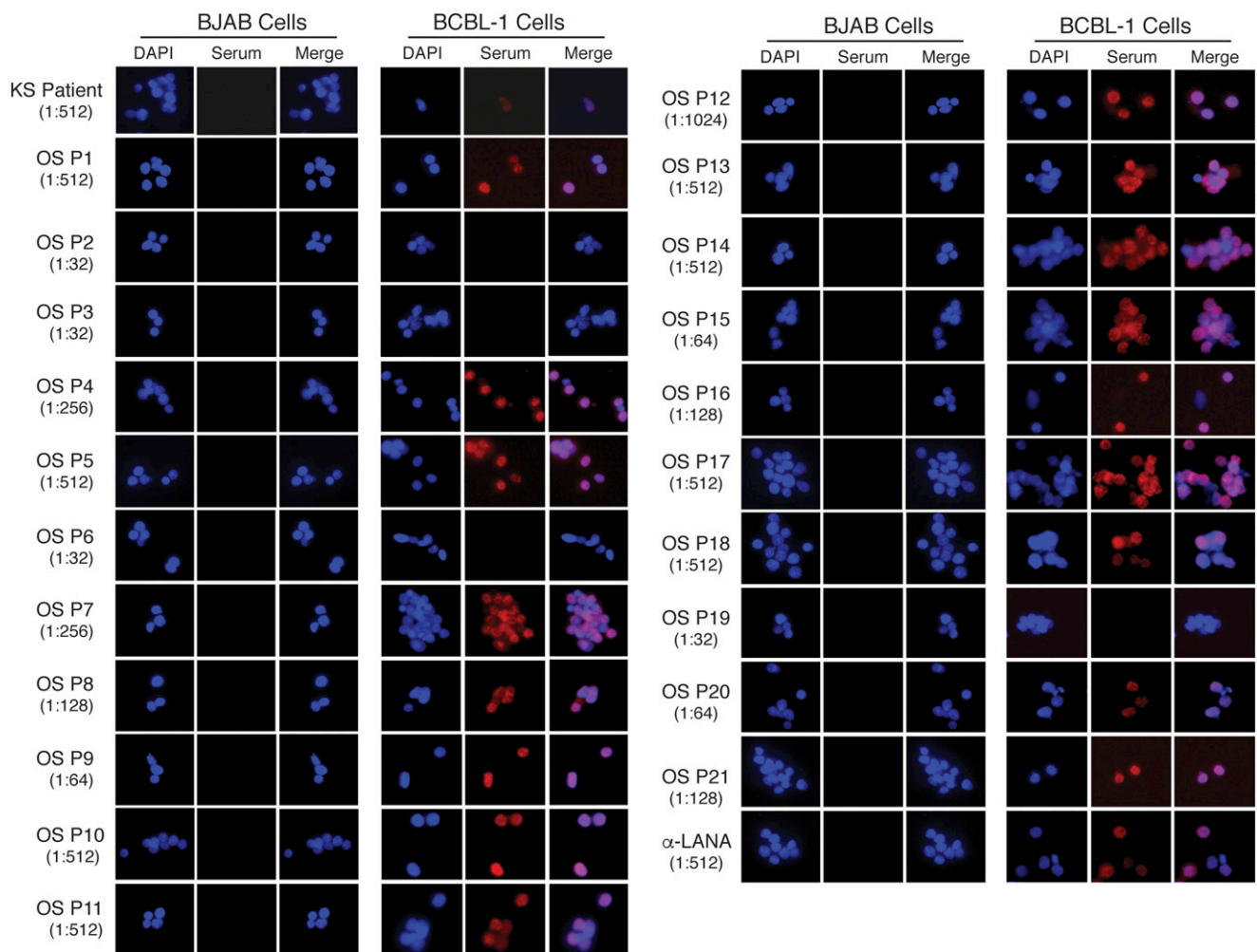


**Fig. 1.** The presence of antibodies specific to KSHV in sera of osteosarcoma patients. Serum samples from 21 Uyghur osteosarcoma patients were examined for KSHV seropositivity with KSHV-negative BJAB and KSHV latently infected BCBL-1 cells. Serum from a KS patient and an anti-LANA antibody were included as positive controls. Sera and antibody were diluted in a twofold serial fashion and reacted with the cells on slides (the dilution for each serum was listed under the patient identity number on the left). No serum was found to react with BJAB cells, but some osteosarcoma sera reacted with BCBL-1 cells showing bright punctate staining in the nuclei, a typical LANA staining reported previously (29). The nuclear punctate staining pattern can also be seen in BCBL-1 cells staining with an anti-LANA antibody illustrated in the last row of the figure.

(Fig. 1). In contrast, the control group sera showed a seropositive rate of 29.4% (Table 1 and *SI Appendix, Table S2*), consistent with the data previously reported (19, 20). The odds ratio (OR = 10.23; 95% CI: 4.25 to 18.89) and *P* value (*P* < 0.0001) indicate that KSHV infection is a risk factor for osteosarcoma occurrence in the Xinjiang Uyghur population.

**The KSHV Genomic DNA and LANA Protein Can Be Detected in Most of the Osteosarcoma Tumors of KSHV-Seropositive Patients.** Surgical specimens of osteosarcoma tumors and adjacent normal tissue samples were obtained from 17 of these 21 patients, including 14 cases of KSHV-seropositive and three seronegative patients. These samples were examined in a blinded fashion for the presence of the KSHV genome (the examiners were unaware of patient identities and sample types). Nested PCR was employed to detect KSHV genomic DNA using five sets of primers targeting viral genes K5, ORF25, ORF26, ORF37, and ORF73 (LANA), respectively (Fig. 2A). Quantitative PCR was also performed using ORF73-specific primers in a blinded fashion (Fig. 2B). With 100% consistency, both assays showed that the KSHV DNA genome was detected in 12 out of 14 tumors from the KSHV-seropositive patients and was absent or below the detection in the tumors of the other two patients, P14 and P16. The KSHV genome was not detected in the tumors of three KSHV-seronegative patients. No KSHV DNA sequence was detected in adjacent normal tissues of all cases, regardless of their KSHV serological status. Two sets of primers for the Epstein-Barr virus (EBV) genome were included in the Nested PCR assay. No EBV DNA was detected in any of these tumors (Fig. 2A).

Osteosarcoma samples from five patients were subjected to immunohistochemical (IHC) analysis for KSHV LANA. P1, P11, P20, and P21 osteosarcomas exhibited intense LANA staining in spindle- or cigar-shaped osteosarcoma cells (Fig. 2C), indicating that these osteosarcoma cells carry latently infected KSHV. The osteosarcoma of P16 did not express LANA, which was consistent with the result that the KSHV genome was not detected in the tumor of this patient.

**Gene Expression Profiling Reveals that KSHV-Positive Osteosarcoma Represents a Distinct Subtype of Osteosarcomas.** Gene expression profiles of the osteosarcoma samples were characterized to reveal a possible role of KSHV in osteosarcoma development. Total RNAs were purified from six KSHV-positive (P1, P5, P9, P11, P20, and P21) and four KSHV-negative osteosarcomas (P2, P3, P14, and P16) along with related adjacent normal tissues (except P2 that lacks its adjacent normal tissue) and subjected to RNA sequencing (RNA-seq) analysis. RNA-seq reads were first mapped to the KSHV genome (GO994935.1) (*SI Appendix, Table S3*) and visualized on a linear scale to provide an overview of highly expressed regions of the genome. At first glance, six KSHV-positive osteosarcomas exhibit two distinct patterns of viral gene expression: 1) P1, P11, and P20 expressed a high level of PAN RNA (polyadenylated nuclear RNA), and 2) P5, P9, and P21 had a relatively low expression level of PAN RNA but a

high expression level of K2 (vIL-6 or viral interleukin-6). In addition, the expression of ORF4, ORF45, and ORF50 (RTA or replication and transcription activator) were also detected in these tumors (Fig. 3A). Therefore, KSHV-positive osteosarcomas can be grouped into two classes based on the viral gene expression profiles, namely the PAN class and the vIL-6 class. The complete range of read depths across the KSHV genome is visualized on a log scale (*SI Appendix, Fig. S1*).

Then, the RNA-seq reads were aligned to the human genome (hg19/GRCh37), and the FPKMs (fragments per kilobase million) were subjected to unsupervised clustering and differential expression analyses. Clustering of cell samples (*x*-axis) and genes (*y*-axis) were performed by hierarchical clustering with average linkage method and Euclidean distance metric (Fig. 3B). The convergence and divergence among these osteosarcomas and their adjacent normal tissues were determined by linkage distance based on the Pearson correlation coefficient and the principal component analysis (PCA). The results show that the gene expression profiles of all 10 osteosarcomas are distinct from the adjacent normal tissues. Four KSHV-negative osteosarcomas are very similar in their gene expression profiles but distantly categorized from KSHV-positive tumors (*P* < 0.05) (Fig. 3C and D), suggesting that KSHV-positive osteosarcomas arose by different pathogenesis than that of nonviral osteosarcomas. Furthermore, KSHV-positive osteosarcomas were divided into two categories visualized by PCA on their cellular gene expression profiles (Fig. 3D). Interestingly, these two categories respectively correspond to the PAN and the vIL-6 classes, suggesting that the different viral gene expression pattern leads to divergent cell reprogramming through either directly affecting host gene expression or changing the environment of host cells.

Differentially expressed genes (DEGs) of osteosarcomas versus their adjacent normal tissues were subjected to a Gene Ontology (GO) analysis to reveal specific and significant associations with specific GO terms. KSHV-positive and -negative osteosarcomas share some common characteristics in gene expression but exhibit more diversity (*SI Appendix, Fig. S2A*). For instance, all subtypes of osteosarcoma exhibit enriched biological process categories “multicellular organism development,” “angiogenesis,” and “extracellular matrix (ECM) organization.” However, “inflammatory response” and “positive regulation of cell migration” are unique to KSHV-positive osteosarcomas, while “DNA repair” and “response to organic substance” terms are only seen in KSHV-negative osteosarcomas (*SI Appendix, Fig. S2 B–D*). Besides, common and unique terms of “biological process” or “molecular function” are also found between two KSHV-positive classes (PAN-class and vIL-6-class) (*SI Appendix, Fig. S2*). It is worth noting that “inflammatory response” is significantly enriched in KSHV-positive osteosarcomas, both PAN-class (2.73% DEGs involved, *P* = 0.006) and vIL-6-class (2.78% DEGs involved, *P* = 0.0021), but not in KSHV-negative osteosarcomas (*SI Appendix, Fig. S2 B–D*). Furthermore, “positive regulation of interferon-gamma production” is uniquely enriched in vIL-6-class (0.67% DEGs involved, *P* = 0.024). These data provide additional evidence of the virus burden in KSHV-positive

**Table 1. Risk of KSHV infection with osteosarcoma occurrence**

	Osteosarcoma (%) ( <i>n</i> = 21)	Control group (%) <sup>*</sup> ( <i>n</i> = 327)	Odds ratio (95% CI)	<i>P</i> value
KSHV-positive	17 (81.0)	96 (29.4)	10.23 (4.25–18.89)	<0.0001
KSHV-negative	4 (19.0)	231 (70.6)		
Total	21 (100.0)	327 (100.0)		

KSHV prevalence in Uyghur osteosarcoma patients = 81.0%. KSHV prevalence in Uyghur general population = 29.4%.

<sup>\*</sup>Control group includes 327 Uyghur donors who came to the hospital for annual physical examination.





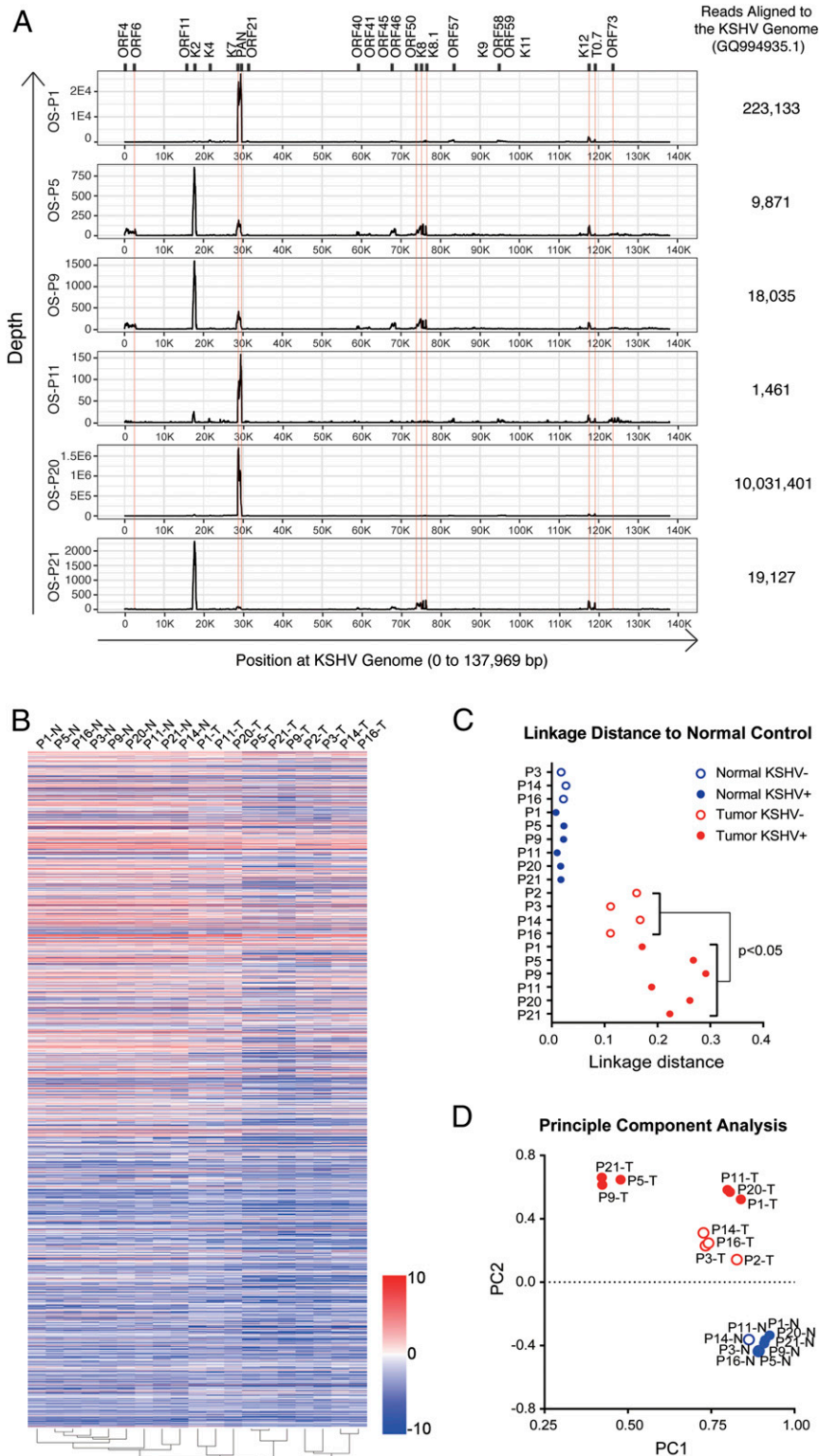


**Fig. 3.** KSHV-positive and -negative osteosarcomas represent distinct subtypes of osteosarcoma on gene expression profiles. (A) KSHV transcriptome of six KSHV-positive osteosarcomas (P1, P5, P9, P11, P20, and P21). RNA-seq reads were aligned to the complete KSHV reference genome (version GQ994935.1) and visualized on a linear scale. The y-axis represents the number of reads aligned to each nucleotide position of the KSHV genome. KSHV genome positions are indicated at the bottom of each panel. Total reads mapped to the KSHV genome of each clinical sample are listed on the right. (B) The RNA-seq reads of 10 osteosarcomas as well as their adjacent normal tissue samples were mapped to the human reference genome (version hg19/GRCh37). Unsupervised clustering of osteosarcoma samples (x-axis) and genes (y-axis) were performed by the average linkage method. (C) Linkage distance to normal tissue was determined by the Pearson correlation coefficient. (D) The first two principal components of these data were identified and shown in a multiple dimensional scaling plot.

**Table 2. Baseline characteristics of Uyghur osteosarcoma patients**

Characteristics	Patient KSHV serostatus (n = 21)			Patient KSHV genomic DNA (n = 17)		
	No. of subjects (%)	KSHV seropositivity (%)	P value	No. of subjects (%)	KSHV DNA-positivity (%)	P value
<b>Gender</b>						
Male	9 (42.9)	9 (100.0)	0.104	8 (47.1)	6 (75.0)	1.00
Female	12 (57.1)	8 (66.7)		9 (52.9)	6 (66.7)	
<b>Age group</b>						
5–30 y	18 (85.7)	15 (83.3)	0.489	14 (82.4)	12 (85.7)	0.024
>30 y	3 (14.3)	2 (66.7)		3 (17.6)	0 (0)	
<b>Diagnosis</b>						
CIMOS*, fibroblastic	3 (14.2)	2 (66.6)	0.962	2 (11.8)	1 (50.0)	0.478
CIMOS, osteoblastic	6 (28.6)	5 (83.3)		4 (23.6)	4 (100.0)	
CIMOS, chondroblastic	2 (9.5)	2 (100.0)		2 (11.8)	2 (100.0)	
CIMOS, myxoid	1 (4.8)	1 (100.0)		0 (0)	0 (0)	
CIMOS, round cell	1 (4.8)	1 (100.0)		1 (5.9)	1 (100.0)	
CIMOS, mixed	5 (23.8)	3 (60.0)		5 (29.4)	2 (40.0)	
CIMOS, NOS <sup>†</sup>	1 (4.8)	1 (100.0)		1 (5.9)	1 (100.0)	
WDIOS <sup>‡</sup>	2 (9.5)	2 (100.0)		2 (11.8)	1 (50.0)	
<b>Tumor location</b>						
Femur	11 (52.3)	9 (81.8)	0.421	8 (47.0)	4 (50.0)	0.109
Tibia	5 (23.8)	5 (100.0)		5 (29.4)	5 (100.0)	
Humerus	2 (9.5)	2 (100.0)		2 (11.8)	2 (100.0)	
Pelvis	1 (4.8)	0 (0)		1 (5.9)	0 (0)	
Clacivle	1 (4.8)	1 (100.0)		1 (5.9)	1 (100.0)	
Scapula	1 (4.8)	1 (100.0)		0 (0)	0 (0)	
<b>Chemotherapy</b>						
Neoadjuvant chemotherapy	15 (71.4)	12 (80.0)	1.00	12 (70.6)	8 (66.7)	1.00
Never	6 (28.6)	5 (83.3)		5 (29.4)	4 (80.0)	
Total	21 (100.0)	17 (81.0)		17 (100.0)	12 (70.6)	

\*CIMOS: conventional intramedullary osteosarcoma.

<sup>†</sup>NOS: no otherwise specified.<sup>‡</sup>WDIOS: well-differentiated intramedullary osteosarcoma.

osteosarcoma does not comprise the majority of osteosarcoma in the Han and other low KSHV prevalence populations, and that KSHV-associated osteosarcoma may not be unique in Uyghur children but can also develop in children of other races who contracted KSHV at an early age. KSHV prevalence is known to be high in specific areas on the globe, such as Eastern African (Uganda, Cameroon, Democratic Republic of Congo, Tanzania, and Zambia). It is very intriguing to know whether the occurrence of childhood osteosarcoma is high in these regions. Since many developing countries do not have cancer registries or many childhood cancers are not diagnosed, there is a lack of epidemiology study for childhood osteosarcoma in these countries. However, a simulation-based study of global childhood cancer suggested that pediatric osteosarcoma in Eastern Africa is several fold higher than in Southern and Northern Africa in parallel with KS (25). On the other hand, the possibility also exists that KSHV-associated osteosarcoma is unique in the Xinjiang Uyghur population, analogous to EBV-associated Burkitt's lymphoma, which is common in African children, and EBV-caused nasopharyngeal carcinoma, which mainly occurs in Southern China. Further investigation is warranted to identify the risk factors associated with the area or population in hope that strategies can be developed to reduce osteosarcoma occurrence, such as preventing children from KSHV infection at an early age.

Osteosarcoma is not a single disease but a collection of neoplasms with different etiologies, sharing a histological hallmark of osseous matrix production in association with malignant cells. Our study showed that KSHV-positive and -negative osteosarcomas exhibit distinct gene expression profiles, implicating that osteosarcomas caused by biological (virus), chemical (carcinogens),

or physical (radiation) agents can be categorized into different subtypes based on their gene expression profiles. Furthermore, KSHV-positive osteosarcomas can be further classified into two distinct classes (the PAN class and the vIL-6 class) based on their viral and cellular gene expression profiles. Further studies are warranted to determine whether these gene signature-defined categories are linked to certain clinical features and osteosarcoma manifestation, which will be of great diagnostic or prognostic significance. On the other hand, it is also important to identify gene signatures for pan-osteosarcomas. For example, TGF- $\beta$ 1/3 and their receptor TGF- $\beta$ R2 were found to be upregulated in all osteosarcomas regardless of KSHV infection status. It is consistent with previous observations that high-grade osteosarcomas have a significantly higher expression of TGF- $\beta$ 1, which may influence the sarcoma's aggressive clinical behavior (26), and that TGF- $\beta$ 3 is associated with disease progression (27). Besides, "multicellular organism development" and "ECM organization" are also found at the top of the significant GO term list for all osteosarcoma samples and present a common feature for all osteosarcomas. Accurate subtype classification and identification of pan-osteosarcoma and subtype-specific markers will dramatically improve our capability to diagnose and treat human osteosarcoma.

## Materials and Methods

**Patients and Participants.** The study included patients with osteosarcoma (age from 5 to 53 y old, median 15 y old) who were admitted and treated in the period of 2016 to 2019 in the Division of Orthopedic Oncology, the First Affiliated Hospital of Xinjiang Medical University, Urumqi, China. Among the patients, the majority was of Uyghur ethnicity (21 Uyghurs, 1 Kazakh, 9 Hans). All patients underwent a core needle biopsy or surgical biopsy for diagnosis. Blood samples were also collected. A total of 15 Uyghur osteosarcoma



patients received 4 to 10 wk neoadjuvant chemotherapy (Doxorubicin, Cisplatin, and Ifosfamide), and 6 were not treated with chemotherapy prior to surgery. Then extensive resection or radical surgery was performed. Surgically removed osteosarcoma tumors and adjacent normal tissues were collected from these patients. Demographic and clinical data are listed in Table 2 and *SI Appendix, Table S1*. Sera were also collected from 327 healthy Uyghur donors who came to the hospital for annual physical examination as reference (*SI Appendix, Table S2*). The human sample collection and the use of clinical samples in the research were approved by the Institutional Review Boards of the Xinjiang Medical University, the First Affiliated Hospital (Approval No. 2018-112903), and Sun Yet-sen University (Approval No. 2015-028). Informed consent was obtained from all osteosarcoma patients (or their guardians) and healthy donors.

**Reagents and Antibodies.** Cell culture media (RPMI1640 and minimum essential medium [MEM]-alpha), streptomycin, penicillin, and TRIzol reagent were purchased from Invitrogen. Nonessential amino acids, glutamine,  $\beta$ -glycerophosphate, dexamethasone, and Alizarin Red S, paraformaldehyde (PFA) were obtained from Sigma-Aldrich. Antibody against LANA (ab4103) was purchased from Abcam. Alexa Fluor 555 goat anti-Human IgG (H+L) antibody (A21433) was purchased from Invitrogen. Alexa Fluor 555 goat anti-Rat IgG antibody (A21434) was purchased from Life Technologies. Hematoxylin (G1004) and eosin (G1002) were obtained from Servicebio technology. HRP-labeled goat anti-rabbit IgG (SP-D2) and DAB (3,3'-diaminobenzidine tetrahydrochloride) reaction kit (DAB-1031) were purchased from Maxim Biotechnologies.

**Expression and Purification of KSHV K8.1, ORF65, and LANA Proteins in *Escherichia Coli*.** cDNAs of KSHV K8.1, ORF65, and LANA were cloned into the pET-28a vector with a hexahistidine (6xHis)-tagged at the N terminus. *Escherichia coli* Rosetta cells were transformed with each of the recombinant plasmids and cultured in LB medium containing 30  $\mu$ g/mL Kanamycin. The expression of these proteins was induced with 1 mM isopropyl  $\beta$ -D-thiogalactoside when the optical density of culture reached OD of 0.6. For K8.1, induced culture was collected after 4 h of cultivation at 16 °C, while for LANA and ORF65, cultures were collected after 4 h of cultivation at 37 °C. Cells were ultrasonicated in lysis buffer containing PMSF (phenylmethylsulfonyl fluoride) without dithiothreitol, and proteins were purified with Ni-NTA column chromatography. Protein concentrations were determined by BCA protein assay kit (Thermo Fisher).

**ELISA.** Purified K8.1, ORF65, and LANA proteins (100  $\mu$ L, 5  $\mu$ g/mL) were respectively coated on ELISA plates (Jet Biofil) in coating buffer (0.1 M NaHCO<sub>3</sub>, pH 9.6 to 10.0) at 4 °C overnight. Plates were saturated with blocking buffer (5% dried skimmed milk in PBS (phosphate-buffered saline) containing 0.1% Tween 20). Each serum in a series of dilutions (1:50 to 1:1,600) reacted with coated plates at 37 °C for 90 min. After washing with PBS-Tween 20 three times, a peroxidase-conjugated anti-human IgG antibody (1:3,000 dilution) was added and incubated at 37 °C for 30 min. Tetramethylbenzidine and hydrogen peroxide substrates were dispensed and incubated in the dark at 37 °C for 15 min. The plates were read at 450 nm (OD450) using a microplate reader (BioTek) with the cutoff for seropositivity of OD450 > 0.5. Before this ELISA system was used to analyze osteosarcoma patient sera, the system had been verified with 21 Uyghur sera with known KSHV serological status (LANA, ORF65m K8.1 seropositivity) (28) with 98.4% consistency and accuracy. Each osteosarcoma patient serum was tested three times in a blinded fashion. An ELISA titer of >1:100 was considered to be positive. To ensure interassay comparability, we used a "highly positive" serum from the previous assay as a positive control and a negative serum from a healthy donor as a negative control.

**Immunofluorescence Assay.** BCBL-1 (KSHV latently infected) and BJAB (KSHV-negative) cells were fixed with 3.6% formaldehyde in PBS and permeabilized with 0.1% Triton X-100. Cells were preincubated with 1% BSA (bovine serum albumin) and then reacted with patient sera in twofold serial dilutions. AIDS-KS patient serum and an anti-LANA antibody (ab4103, Abcam) were included as positive controls. Alexa Fluor555 goat anti-human IgG (1:500 dilution) was used as the secondary antibody (Alexa Fluor555 goat anti-Rat IgG for anti-LANA control). Cells were visualized under a Zeiss Observer Z1 fluorescence microscope. The assay was done in a blinded manner, and the serum yielding the nuclear punctate pattern in >1:64 dilution was considered positive.

**PCR Analyses.** Total DNA was extracted from each tumor or adjacent normal tissue sample using a HiPure Tissue DNA Mini Kit (Magen). A total of 200 ng of each DNA was subjected to nested PCR. The oligonucleotide primers for the first- and second-round PCR for KSHV K5, ORF25, ORF26, ORF37, ORF73 (LANA), EBV LMP1, and EBNA1 were listed in *SI Appendix, Table S5*. PCR was

performed in a 50- $\mu$ L volume reaction (0.4  $\mu$ M primers and 2xPrimeSTAR HS [Premix], 5% dimethyl sulfoxide) as follows: denaturing at 95 °C for 5 min, 25 cycles of reaction (95 °C for 30 s, 55 to 62 °C for 30 s, and 72 °C for 30 s), and final elongation of 72 °C for 7 min. PCR was carried out in a blinded fashion (the examiner was unaware of patient identities and sample types). Each sample was tested three times independently.

**Quantitative Real-Time PCR and qRT-PCR Analyses.** A total of 200 ng purified tissue DNA was subjected to quantitative real-time PCR with KSHV ORF73 primers and SYBR Green Master Mix (Thermo Fisher) on LightCycler 480II (Roche). LANA standard DNA in serial dilutions were analyzed simultaneously with osteosarcoma DNAs for a standard curve. KSHV genomic DNA copy numbers of initial specimens were calculated according to the standard curve. The lowest standard DNA copy number used to construct the standard curve (10 DNA copies) still exhibited a positive peak and was in the linear range in the standard curve, so 10-copy is set to be the sensitive line for our assay. Cycle threshold (Ct) value cutoff is 35 cycles. For the quantification of RNA, total RNA was isolated using TRIzol reagent (Invitrogen). RNA concentration was measured by Nanodrop 2000 (Thermo Fisher). A total of 500 ng RNA was reverse transcribed into cDNA followed by RT-PCR with SYBR Green Master Mix and specific primers on LightCycler 480II. The primer sequences used are listed in *SI Appendix, Table S5*.

**IHC Analysis.** Osteosarcoma clinical samples were fixed in 4% PFA and decalcified in 10% EDTA/0.2% PFA in PBS in microwave decalcifying apparatus. Complete decalcification was verified by X-ray images. Tumor samples including Osteosarcoma, KS, and Lymphangioma were impregnated in paraffin, and sections were subjected to hematoxylin and eosin and IHC staining. For IHC, after removal of endogenous peroxidase with 3% H<sub>2</sub>O<sub>2</sub> and rinsing in PBS, sections were incubated with an antibody against LANA (ab4103, Abcam) in 1:100 dilution at 4 °C overnight. A goat anti-rabbit HRP secondary antibody (DAB-1031, Maxim) was used, followed by metal-enhanced DAB colorimetric detection. Then, sections were counterstained with hematoxylin.

**RNA-seq.** Osteosarcoma tumors and adjacent normal tissues were lysed, and total RNA was extracted with TRIzol reagent. DNA contamination was eliminated by DNase I treatment. RNA purity was determined using the Qubit 3.0 Fluorometer (Life Technologies). For each sample, 1 to 3  $\mu$ g RNA was used to generate sequencing libraries with NEBNext Ultra RNA Library Prep Kit for Illumina (#E7530L, NEB) with poly(A) Magnetic Isolation Module (NEB #7490). Fragmentation was carried out using divalent cations under elevated temperature in NEBNext first-strand synthesis reaction buffer. First-strand cDNA was synthesized using random hexamer primer and RNase H. Second-strand cDNA was synthesized using DNA polymerase I and RNase H. The library fragments were purified with QiaQuick PCR kits. Index codes were added to attribute sequences to each sample. The libraries were sequenced on an Illumina HiSeq 4000 platform, and 150 bp paired-end reads were generated.

**Data Process.** Raw data in FASTQ format were filtered, mapped, and analyzed as before. Briefly, the short reads were aligned to the KSHV reference genome (version GQ994935.1) and the human reference genome (version hg19/GRCh37). The quality of raw data was viewed by multiQC. The number of clean tags mapped to each gene was counted by FPKM reads. Corrected *P* value (*Q* value) < 0.05 and |log<sub>2</sub> (fold change)| > 1 were set as the threshold for significantly different expression.

**Data Analysis.** GO analysis was performed with GO tools (<http://geneontology.org/>), and GO terms with *P* < 0.05 were considered as significantly enriched gene sets. Venn diagrams were drawn by Venny 2.0 online (<https://bioinfo.pcnb.cic.es/tools/venny/index.html>). Unsupervised clustering of samples (*x*-axis) was performed with the average linkage method and Euclidean distance metric, respectively. Linkage distance was performed by calculating the Pearson correlation coefficient with normal control and then subtracted by 1. Gene Set Enrichment Analysis (GSEA) was performed using GSEA-3.0 software between osteosarcoma tumor and adjacent normal tissue samples with 2,000 of "Geneset" permutations type and default values for other parameters. FPKM and RPKM values of RNA expression were used in this analysis. KEGG, Reactome, and hallmark gene sets were used in this analysis (<https://www.gsea-msigdb.org/gsea/msigdb/collections.jsp>). All differentially expressed pathways with FDR (false discovery rate) *q* value < 0.1 were kept for subsequent analysis.

**Statistical Analyses.** Data were analyzed with SPSS 25.0 program. Fisher's exact test was used to analyze baseline data. The OR was calculated to estimate the association between KSHV infection and osteosarcoma occurrence. Woolf's method was applied to calculate a 95% CI.  $P < 0.05$  was considered significant.

**Data Availability.** RNA-seq data have been deposited in the NCBI (National Center for Biotechnology Information) GEO (Gene Expression Omnibus)

database ([GSE126209](https://doi.org/10.1093/nar/gkz126209)). All other study data are included in the article and/or supporting information.

**ACKNOWLEDGMENTS.** We thank Yuan Lab members for discussion, constructive suggestions, and participation in blinded serological and quantitative PCR experiments. The research reported in this publication was supported by the Natural Science Foundation of China (81530069).

1. T. A. Damron, W. G. Ward, A. Stewart, Osteosarcoma, chondrosarcoma, and Ewing's sarcoma: National cancer data base report. *Clin. Orthop. Relat. Res.* **459**, 40–47 (2007).
2. L. Mirabello, R. J. Troisi, S. A. Savage, International osteosarcoma incidence patterns in children and adolescents, middle ages and elderly persons. *Int. J. Cancer* **125**, 229–234 (2009).
3. L. U. Gardner, H. F. Heslington, Osteosarcoma from intravenous beryllium compounds in rabbits. *Fed. Proc.* **5**, 221 (1946).
4. M. F. Stanton, Primary tumors of bone and lung in rats following local deposition of cupric-chelated N-hydroxy-2-acetylaminofluorene. *Cancer Res.* **27**, 1000–1006 (1967).
5. P. M. Hatfield, M. D. Schulz, Postirradiation sarcoma. Including 5 cases after X-ray therapy of breast carcinoma. *Radiology* **96**, 593–602 (1970).
6. M. Arlen *et al.*, Radiation-induced sarcoma of bone. *Cancer* **28**, 1087–1099 (1971).
7. M. P. Finkel, B. O. Biskis, P. B. Jinkins, Virus induction of osteosarcomas in mice. *Science* **151**, 698–701 (1966).
8. M. P. Finkel, B. O. Biskis, C. Farrell, Osteosarcomas appearing in Syrian hamsters after treatment with extracts of human osteosarcomas. *Proc. Natl. Acad. Sci. U.S.A.* **60**, 1223–1230 (1968).
9. Y. Chang *et al.*, Identification of herpesvirus-like DNA sequences in AIDS-associated Kaposi's sarcoma. *Science* **266**, 1865–1869 (1994).
10. K. Antman, Y. Chang, Kaposi's sarcoma. *N. Engl. J. Med.* **342**, 1027–1038 (2000).
11. L. Giffin, B. Damania, KSHV: Pathways to tumorigenesis and persistent infection. *Adv. Virus Res.* **88**, 111–159 (2014).
12. J. N. Martin, "The epidemiology of KSHV and its association with malignant disease" in *Human Herpesviruses: Biology, Therapy, and Immunoprophylaxis*, A. Arvin, Ed. *et al.* (Cambridge University Press, Cambridge, 2007), pp. 960–985.
13. Y. Li *et al.*, Evidence for Kaposi's sarcoma originating from Mesenchymal stem cell through KSHV-induced Mesenchymal-to-Endothelial Transition. *Cancer Res.* **78**, 230–245 (2018).
14. C. H. Parsons, B. Szomju, D. H. Kedes, Susceptibility of human fetal mesenchymal stem cells to Kaposi sarcoma-associated herpesvirus. *Blood* **104**, 2736–2738 (2004).
15. M. S. Lee *et al.*, Human mesenchymal stem cells of diverse origins support persistent infection with Kaposi's sarcoma-associated herpesvirus and manifest distinct angiogenic, invasive, and transforming phenotypes. *MBio* **7**, e02109–e02115 (2016).
16. J. Naipauer *et al.*, PDGFRA defines the mesenchymal stem cell Kaposi's sarcoma progenitors by enabling KSHV oncogenesis in an angiogenic environment. *PLoS Pathog.* **15**, e1008221 (2019).
17. A. J. Mutsaers, C. R. Walkley, Cells of origin in osteosarcoma: Mesenchymal stem cells or osteoblast committed cells? *Bone* **62**, 56–63 (2014).
18. A. Abarrategi *et al.*, Osteosarcoma: Cells-of-origin, cancer stem cells, and targeted therapies. *Stem Cells Int.* **2016**, 3631764 (2016).
19. P. Dilnur *et al.*, Classic type of Kaposi's sarcoma and human herpesvirus 8 infection in Xinjiang, China. *Pathol. Int.* **51**, 845–852 (2001).
20. T. Zhang *et al.*, Human herpesvirus 8 seroprevalence, China. *Emerg. Infect. Dis.* **18**, 150–152 (2012).
21. Y. Yang, J. Chen, H. Chu, T. Wang, X. Song, Epidemiological features analysis of uighur, han and Kazak patients with osteosarcoma in Xinjiang area. *J. Pract. Orthop.* **24**, 130–133 (2018).
22. B. Fuchs, D. J. Pritchard, Etiology of osteosarcoma. *Clin. Orthop. Relat. Res.* **397**, 40–52 (2002).
23. Y. Cao *et al.*, High prevalence of early childhood infection by Kaposi's sarcoma-associated herpesvirus in a minority population in China. *Clin. Microbiol. Infect.* **20**, 475–481 (2014).
24. S. de Sanjose *et al.*, Geographic variation in the prevalence of Kaposi sarcoma-associated herpesvirus and risk factors for transmission. *J. Infect. Dis.* **199**, 1449–1456 (2009).
25. Z. J. Ward, J. M. Yeh, N. Bhakta, A. L. Frazier, R. Atun, Estimating the total incidence of global childhood cancer: A simulation-based analysis. *Lancet Oncol.* **20**, 483–493 (2019).
26. A. Franchi *et al.*, Expression of transforming growth factor beta isoforms in osteosarcoma variants: Association of TGF beta 1 with high-grade osteosarcomas. *J. Pathol.* **185**, 284–289 (1998).
27. P. Kloen *et al.*, Expression of transforming growth factor-beta (TGF-beta) isoforms in osteosarcomas: TGF-beta3 is related to disease progression. *Cancer* **80**, 2230–2239 (1997).
28. J. Zheng *et al.*, Prevalence of Kaposi's sarcoma-associated herpesvirus in Uygur and Han populations from the Urumqi and Kashgar regions of Xinjiang, China. *Virol. Sin.* **32**, 396–403 (2017).
29. D. H. Kedes *et al.*, The seroepidemiology of human herpesvirus 8 (Kaposi's sarcoma-associated herpesvirus): Distribution of infection in KS risk groups and evidence for sexual transmission. *Nat. Med.* **2**, 918–924 (1996).